

Phase Transitions and Molecular Motions in Guanidinium- d_6 Trihalogenomercurates(II) $[\text{C}(\text{ND}_2)_3]\text{HgBr}_3$ and $[\text{C}(\text{ND}_2)_3]\text{HgI}_3$ as Investigated by Means of ^{81}Br and ^{127}I NQR and ^2H NMR

Koji Yamada,¹ Hiromitsu Terao,^{*2} Kazuko Sumimura,²
Masao Hashimoto,³ Hiroshi Ohki,⁴ and Tsutomu Okuda⁵

¹Department of Applied Molecular Chemistry, College of Industrial Technology, Nihon University, Narashino 275-8575

²Department of Chemistry, Faculty of Integrated Arts and Sciences, Tokushima University,
Minamijosanjima-cho, Tokushima 770-8502

³Department of Chemistry, Faculty of Science, Kobe University, Nada-ku, Kobe 657-8501

⁴Department of Chemistry, Faculty of Science, Shinshu University, Matsumoto 390-8621

⁵Department of Bio-Recycling, Faculty of Engineering, Hiroshima Kokusai Gakuin University,
Aki-ku, Hiroshima 739-0321

Received October 31, 2006; E-mail: terao@ias.tokushima-u.ac.jp

The temperature dependence of ^2H NMR spectra and ^{81}Br and ^{127}I NQR frequencies was investigated for the deuterated compounds of $[\text{C}(\text{NH}_2)_3]\text{HgBr}_3$ and $[\text{C}(\text{NH}_2)_3]\text{HgI}_3$ between 77 and ca. 400 K. Due to deuteration, the phase-transition temperatures of the iodine compound were increased by 2 and 6 K for the second-order (251 K) and the first-order (210 K) phase transitions, respectively. Distinctive ^{127}I NQR frequency-shifts of more than 200 kHz were observed in the intermediate phase of the iodine compound on deuteration. The temperature dependences of the ^2H NMR spectra for $[\text{C}(\text{ND}_2)_3]\text{HgBr}_3$ and $[\text{C}(\text{ND}_2)_3]\text{HgI}_3$ could be explained by invoking C_3 reorientation of the guanidinium cation. The activation energies for the reorientation evaluated from ^2H NMR were consistent with the former ^1H NMR T_1 results with the exception of the low-temperature phase of the iodine compound. The quite low activation energy from ^2H NMR spectrum for this phase may indicate that the quenching of the orientation disordering of the cations is responsible for the fade-out phenomenon in the ^{127}I NQR resonance lines below ca. 100 K.

It is well known that many halogenometallates with alkylammonium cations undergo phase transitions associated with the molecular motions of the cations.¹ In a previous paper,² we have for the first time reported the occurrence of phase transitions in the $[\text{C}(\text{NH}_2)_3]\text{HgI}_3$ crystals, whereas there are no signs of phase transitions in $[\text{C}(\text{NH}_2)_3]\text{HgBr}_3$. The crystal structure at room temperature of $[\text{C}(\text{NH}_2)_3]\text{HgBr}_3$ ² has a monoclinic $C2/c$ space group and is isomorphous with $[\text{C}(\text{NH}_2)_3]\text{HgI}_3$ ² and $[\text{C}(\text{NH}_2)_3]\text{CdBr}_3$.³ The structure can be described as consisting of a discrete $[\text{C}(\text{NH}_2)_3]^+$ ion and a pseudo one-dimensional polymeric anion chain $(\text{HgBr}_3^-)_\infty$. Each anion chain is formed by two-edges sharing among the adjacent trigonal bipyramids of HgBr_5 , in which a central Hg atom is coordinated by three Br atoms of an HgBr_3^- ion in equatorial positions and two Br atoms intermolecular-connected in apical positions. The crystal structure is stabilized by networks of N–H...Br hydrogen bonds between the cations and the polyanions as well as the electrostatic forces.

Of the above isomorphous series of compounds, it has been found that only $[\text{C}(\text{NH}_2)_3]\text{HgI}_3$ undergoes solid-state phase transitions in the temperature range from 77 to ca. 400 K showing a second-order-type phase transition at $T_{c1} = 251$ K and a first-order-type transition at $T_{c2} = 210$ K. The solid state of $[\text{C}(\text{NH}_2)_3]\text{HgI}_3$ is therefore characterized as having at least

three phases as denoted: room-temperature phase (RTP, $T > T_{c1}$), intermediate temperature phase (ITP, $T_{c1} > T > T_{c2}$), and low-temperature phase (LTP, $T < T_{c2}$). In previous work,² we have also reported that the temperature dependence curves of ^1H NMR T_1 of both $[\text{C}(\text{NH}_2)_3]\text{HgBr}_3$ and $[\text{C}(\text{NH}_2)_3]\text{HgI}_3$ are explainable by invoking C_3 reorientation about the pseudo three-fold axes of the $[\text{C}(\text{NH}_2)_3]^+$ ions. The activation energies of this motion have been estimated to be 35.0 kJ mol^{−1} for the bromine compound, whereas they are 24.1, 30.1, and 23.0 kJ mol^{−1} for RTP, ITP, and LTP, respectively, for the iodine compound. The smaller activation energies in the iodine compound indicate the ease of motion over that in the bromine compound. It is also remarkable that the activation energy in the ITP phase is rather large compared to those in the other phases.

In accordance with the crystal structures, two NQR resonance lines due to ^{81}Br and ^{127}I ($m = 1/2 \leftrightarrow 3/2$) are detected in the bromine compound and in RTP of the iodine compound. Though the temperature dependence of NQR frequencies is normal except for that in ITP of the iodine compound, in which a salient dependence is found. The terminal iodine line shows no practical temperature dependence in this phase, while the bridging iodine one a steep increase with decreasing temperatures. Thus, the above distinctive observations in the

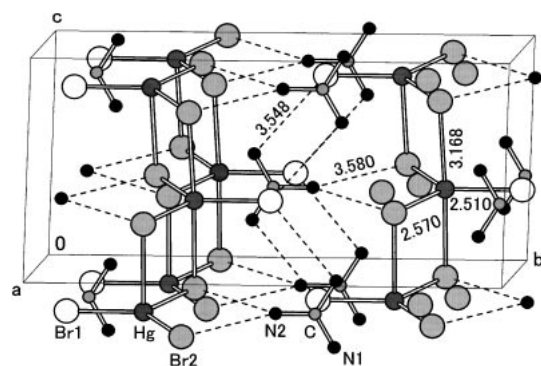


Fig. 1. The crystal structure of $[\text{C}(\text{NH}_2)_3]\text{HgBr}_3$ without H atoms.² Monoclinic ($C2/c$), $Z = 4$, $a = 7.750(2) \text{ \AA}$, $b = 15.646(2) \text{ \AA}$, $c = 7.727(2) \text{ \AA}$, $\beta = 109.12(2)^\circ$. Possible H-bonds $\text{N}-\text{H}\cdots\text{Br}$ are shown with dashed lines.

activation energies from the ^1H NMR T_1 and in the temperature dependence of the NQR frequencies in ITP seem to indicate an occurrence of some dynamical structural change in this phase. To get further information about the cation dynamics, we measured the ^2H NMR spectra of the deuterated compounds $[\text{C}(\text{ND}_2)_3]\text{HgBr}_3$ and $[\text{C}(\text{ND}_2)_3]\text{HgI}_3$ in this study. ^{81}Br and ^{127}I NQR and differential thermal analysis (DTA) measurements were also carried out in order to investigate possible deuteration effects.

Experimental

The partially deuterated compounds $[\text{C}(\text{ND}_2)_3]\text{HgX}_3$ ($X = \text{Br}$ and I) were prepared by mixing equimolar amounts of $[\text{C}(\text{ND}_2)_3]\text{X}$ and HgBr_2 in methanol-OD (CH_3OD ; Nacalai Tesque, Inc. 99% D) followed by evaporation of the solvent for crystallization. The degree of deuteration was determined to be $>90\%$ from the IR spectra. The $[\text{C}(\text{ND}_2)_3]\text{X}$ crystals were obtained by repeated cycles (4 times) of dissolution of the crystals into D_2O (Nacalai Tesque, Inc. 99.8% D) and evaporation of the solvent. All of the deuteration processes were done under N_2 gas atmosphere in a globe bag. The $[\text{C}(\text{NH}_2)_3]\text{X}$ crystals were prepared by neutralizing an aqueous solution of $[\text{C}(\text{NH}_2)_3]_2\text{CO}_3$ with HBr .

NQR spectra were measured on a super-regenerative spectrometer. The signals were recorded on a recorder through a lock-in amplifier with Zeeman modulation. The accuracy of frequency measurement was estimated to be within $\pm 0.02 \text{ MHz}$.

^2H NMR powder spectra were recorded at 41.6 MHz (6.37 T). The measurements were carried out by means of a homemade spectrometer using a solid-echo technique ($\pi/2_x - \pi/2_y$ -echo), followed by a Fourier transformation of the echo signal. The typical $\pi/2$ pulse length and the separation between two $\pi/2$ pulses were 3 and 30–50 μs , respectively. Spectral simulation for ^2H NMR was done by using MXQET.⁴

The DTA measurement was carried out on a homemade apparatus.

Results and Discussion

Deuteration Effects as Found in DTA and NQR Measurements. Figure 1 shows the crystal structure of $[\text{C}(\text{NH}_2)_3]\text{HgBr}_3$ at room temperature (298 K). The crystal is monoclinic $C2/c$ with $Z = 4$, $a = 7.750(2) \text{ \AA}$, $b = 15.646(2) \text{ \AA}$, $c = 7.727(2) \text{ \AA}$, and $\beta = 109.12(2)^\circ$. The $[\text{C}(\text{NH}_2)_3]^+$ ions are in the voids between anion chains $(\text{HgBr}_3^-)_\infty$. Two bridg-

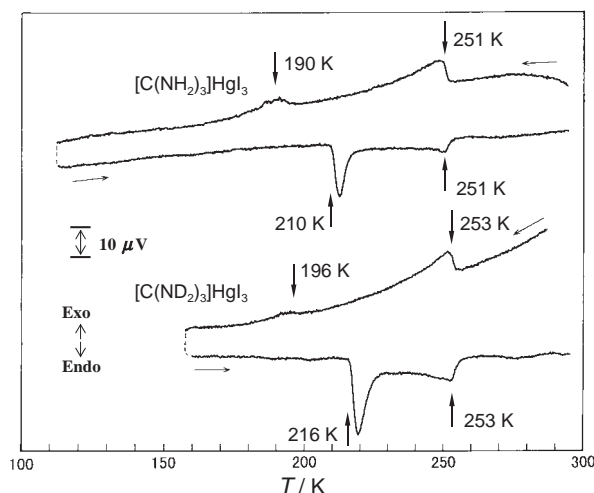


Fig. 2. A representative DTA curve of $[\text{C}(\text{ND}_2)_3]\text{HgI}_3$ together with that of $[\text{C}(\text{NH}_2)_3]\text{HgI}_3$.

ing Br atoms of an HgBr_3^- ion, being crystallographically equivalent, participate in the double chains of $\text{Br}-\text{Hg}-\text{Br}$ by intermolecular $\text{Hg}\cdots\text{Br}$ bonds. The almost flat planes of the $[\text{C}(\text{NH}_2)_3]^+$ ion and the HgBr_3^- ion are tilted by ca. 60° to each other. Short $\text{N}\cdots\text{Br}$ distances of 3.548 for terminal Br atoms and 3.580 \AA for the bridging Br atoms suggest that these atoms may participate in weak $\text{N}-\text{H}\cdots\text{Br}$ hydrogen bonds.^{5,6} The crystal structure of $[\text{C}(\text{NH}_2)_3]\text{HgI}_3$ has been found isomorphous at room temperature with a larger unit cell: $C2/c$, $Z = 4$, $a = 8.424(6) \text{ \AA}$, $b = 16.096(6) \text{ \AA}$, $c = 8.335(7) \text{ \AA}$, and $\beta = 109(1)^\circ$. Though the crystal structures of $[\text{C}(\text{NH}_2)_3]\text{HgI}_3$ at low temperatures have not been reported, the continuous changes at T_{c1} and the splitting pattern at T_{c2} in the ^{127}I NQR frequencies, as shown later, shows that these structures are closely related to and not so different from the room temperature structure.

A representative DTA curve of $[\text{C}(\text{ND}_2)_3]\text{HgI}_3$ is compared to that of $[\text{C}(\text{NH}_2)_3]\text{HgI}_3$ ² in Fig. 2. Though both curves for these compounds were recorded without precise temperature control, the cooling rates were about 1 K min^{-1} , and the heating rate was about 5 K min^{-1} (The differential scanning calorimetry (DSC) curve of the protonated compound which was recorded (using Mac science DSC3100s) with the rates of 10 K min^{-1} for both cooling and heating runs was basically same as the corresponding curve in the figure.). It is obvious that the thermal behavior of the D-compound is only slightly different from that of the H-analogue. That is, a small anomaly with a long tail on the low-temperature side with a peak maximum at $T_{c1}(\text{D}) = 253 \text{ K}$ was observed in both cooling and heating runs. In addition, smeared peaks were always found around 196 K on cooling runs, which suggests that the $\text{ITP} \rightarrow \text{LTP}$ transition occurred gradually in the wide temperature range of the super cooled state. On the other hand, during heating runs, the $\text{LTP} \rightarrow \text{ITP}$ transition always gave sharp peaks, from which we deduced $T_{c2}(\text{D}) = 216 \text{ K}$. The present DTA measurements have shown that increases in both the second-order-type (T_{c1}) and the first-order-type phase-transition temperatures (T_{c2}), which were 2 and 6 K for the former and the latter, respectively, occur upon deuteration.

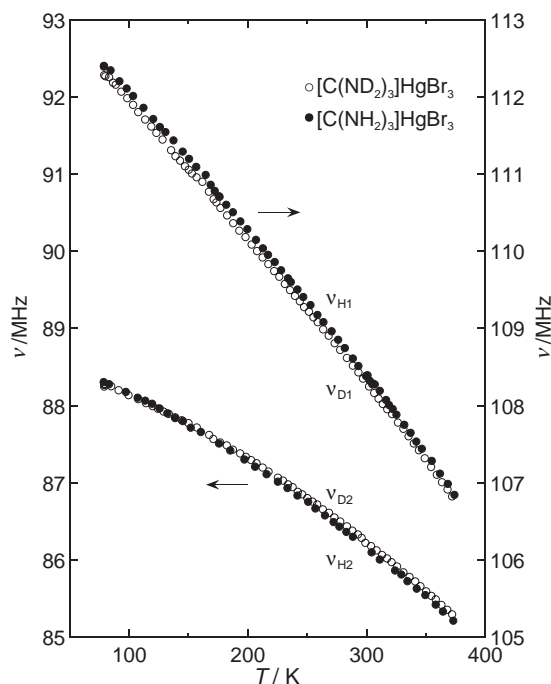


Fig. 3. Temperature dependence of ^{81}Br NQR frequencies of $[\text{C}(\text{ND}_2)_3]\text{HgBr}_3$ (○) together with $[\text{C}(\text{NH}_2)_3]\text{HgBr}_3$ (●).

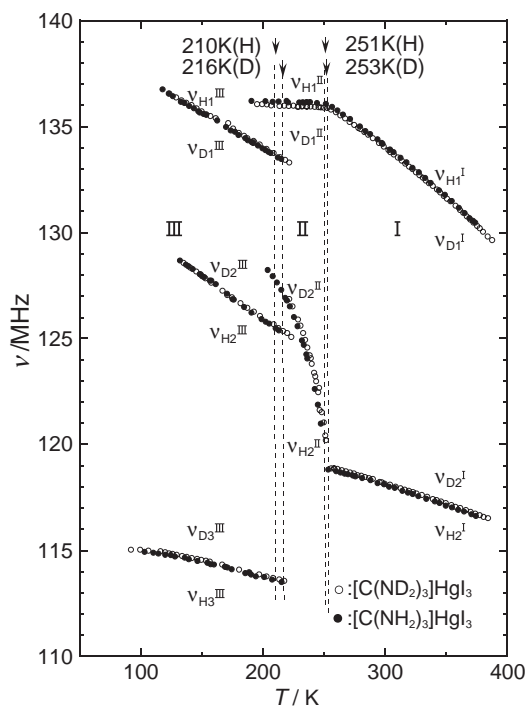


Fig. 4. Temperature dependence of ^{127}I ($m = \pm 1/2 \leftrightarrow \pm 3/2$) NQR frequencies of $[\text{C}(\text{ND}_2)_3]\text{HgI}_3$ (○) together with $[\text{C}(\text{NH}_2)_3]\text{HgI}_3$ (●). Each phase of RTP, ITP, and LTP is denoted by I, II, and III, respectively.

Table 1. ^{81}Br and ^{127}I ($m = \pm 1/2 \leftrightarrow \pm 3/2$) NQR Frequencies of $[\text{C}(\text{ND}_2)_3]\text{HgBr}_3$ and $[\text{C}(\text{ND}_2)_3]\text{HgI}_3$ at Representative Temperatures as Listed Together with Those for the Protonated Compounds

Compound	Nucleus	Phase	T/K	ν/MHz		$\Delta\nu_{\text{D-H}}/\text{MHz}^{\text{b)}$
				D-compd	H-compd ^{a)}	
$[\text{C}(\text{ND}_2)_3]\text{HgBr}_3$	^{81}Br		77	112.23	112.40	−0.17
				88.26	88.31	−0.05
			298	108.32	108.41	−0.09
				86.25	86.17	0.08
$[\text{C}(\text{ND}_2)_3]\text{HgI}_3$	^{127}I	LTP	140	136.03	135.96	0.07
				128.37	128.38	−0.01
				114.69	114.60	0.09
		ITP	235	135.95	136.15	−0.20
				124.82	124.38	0.44
		RTP	298	134.08	134.19	−0.11
				118.21	118.13	0.08

a) Ref. 2. b) $\Delta\nu_{\text{D-H}}$ denotes a frequency difference between the deuterated and protonated compounds.

The temperature dependence of ^{81}Br NQR frequencies of $[\text{C}(\text{ND}_2)_3]\text{HgBr}_3$ is shown together with that of $[\text{C}(\text{NH}_2)_3]\text{HgBr}_3$ in Fig. 3. The lower-frequency line $\nu_{\text{D}2}$ ($\nu_{\text{H}2}$) was almost twice as intense as the higher-frequency line $\nu_{\text{D}1}$ ($\nu_{\text{H}1}$); they were assigned to the bridging and the terminal Br atoms, respectively. Both lines exhibited normal negative temperature dependence without showing any evidence for the occurrence of phase transition. As listed in Table 1, an isotope effect on frequency $\Delta\nu_{\text{D-H}}$, which denotes a frequency difference between the deuterated and protonated compounds, was found up to ca. 200 kHz. Such $\Delta\nu_{\text{D-H}}$ values were also encountered in $(\text{CH}_3\text{NH}_3)_2\text{HgBr}_4$ ⁷ and $\text{CH}_3\text{CH}_2\text{NH}_3\text{HgBr}_3$,⁸ which may

indicate the existence of weak N–H...Br hydrogen-bonding interactions in these crystals. The sign of $\Delta\nu_{\text{D-H}}$ for the terminal Br atoms was negative throughout the measured temperature range, and its absolute value increased with decreasing temperatures. On the other hand, the sign of $\Delta\nu_{\text{D-H}}$ for the bridging Br atoms was positive except for at low temperatures, and its absolute value tended to be larger at high temperatures.

The temperature dependence of the ^{127}I ($m = 1/2 \leftrightarrow 3/2$) NQR frequencies of $[\text{C}(\text{ND}_2)_3]\text{HgI}_3$ is shown in Fig. 4. In this figure, I, II and III denote the room-temperature phase (RTP), the intermediate-temperature phase (ITP), and the low-temperature phase (LTP), respectively. The highest-frequency

lines in each phase, ν_{D1}^I (ν_{H1}^I), ν_{D1}^{II} (ν_{H1}^{II}), and ν_{D1}^{III} (ν_{H1}^{III}), were assigned to the terminal I atom, and the remaining lines, ν_{D2}^I (ν_{H2}^I), ν_{D2}^{II} (ν_{H2}^{II}), ν_{D2}^{III} (ν_{H2}^{III}), ν_{D3}^{III} (ν_{H3}^{III}), were assigned to the bridging I atoms.² On the phase transition from RTP to ITP, both ν_{D1}^I and ν_{D2}^I changed continuously without showing any jumps, in accordance with a second-order phase-transition nature. On the other hand, on going from ITP to LTP clear jumps between resonance lines of both phases, in accordance with a first-order-type phase-transition nature, were observed. Superheating as well as supercooling in the NQR frequency measurements were observed at the $T_{c2}(D)$ transition, as seen for the H-compound.² The lower two lines in LTP were situated symmetrically in frequency from an extrapolated line of the lower frequency curve in RTP. Unrecognizable intensity changes occurred between ν_{D1}^I (ν_{H1}^I) and ν_{D1}^{II} (ν_{H1}^{II}) at T_{c1} , whereas both ν_{D2}^I (ν_{H2}^I) and ν_{D2}^{II} (ν_{H2}^{II}) became broader and weaker and were unobservable near T_{c1} . Further, the signal intensities of ν_{D2}^{II} (ν_{H2}^{II}) were rather weak compared to those of ν_{D1}^I (ν_{H1}^I), even if the former lines were subjected very steep temperature dependence. It then seems plausible that another line in ITP exists, which may be situated symmetrically from ν_{D2}^{II} (ν_{H2}^{II}), and its frequency decreases with a decrease in the temperature, as seen for $C_6H_5NHSbX_4$ ($X = Br$ and Cl).⁹ We tried therefore to search the signals for the counter atoms in the expected frequency regions repeatedly, but no signals were detected. It is still not certain whether signals for the counter atoms exist or not. A fade-out phenomenon of the resonance lines accompanied by signal broadening below ca. 100 K in LTP was also observed for $[C(ND_2)_3]HgI_3$, as in the case of the protonated compound (The samples that were slowly cooled and expected to show a complete transformation into the LTP phases gave no signals.). It is notable that relatively large $|\Delta\nu_{D-H}|$ values were observed for both lines in ITP, whereas those in RTP and LTP were relatively small. The $\Delta\nu_{D-H}$ values for the iodine compound, as a whole, appear similar to the bromine compound, which showed negative and positive values for the terminal and the bridging I atoms, respectively. The large $|\Delta\nu_{D-H}|$ values in ITP compared to those in the other phases seem again to be indicative of the occurrence of a dynamical structural change in this phase, which may reflect the difference between N–D...I and N–H...I.

Cation Motions as Investigated by 2H NMR Measurements. Figure 5 shows the 2H NMR T_1 vs. $1/T$ plot at 41.637 MHz of $[C(ND_2)_3]HgBr_3$, which was measured for comparison with the protonated compound. The planar $[C(NH_2)_3]^+$ ions have often been found to undergo a C_3 reorientation motion in crystals.^{2,10–13} In accordance with this, a simple V-shaped T_1 curve was also obtained for the deuterated compound. The curve exhibited a single minimum of 6.5 ms at 339 K, whereas the corresponding one for 1H NMR² at 32 MHz of the protonated compound exhibited a single minimum of 27 ms at 342 K. The following BPP-type equation can be used to analyze the C_3 reorientation of the $[C(ND_2)_3]^+$ ions:

$$\frac{1}{T_1} = C_Q \left(\frac{\tau}{1 + \omega^2 \tau^2} + \frac{4\tau}{1 + 4\omega^2 \tau^2} \right), \quad (1)$$

$$\text{and } \tau = \tau_0 \exp\left(\frac{E_a}{RT}\right), \quad (2)$$

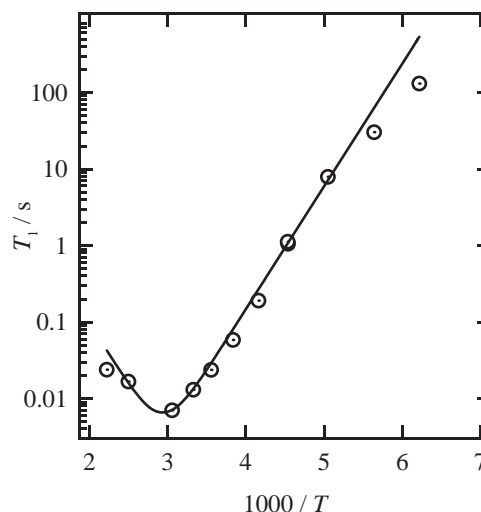


Fig. 5. Temperature dependence of 2H NMR T_1 of $[C(ND_2)_3]HgBr_3$.

where ω is the angular NMR frequency, C_Q is a constant associated with the reduction of the quadrupole coupling constant under this motion, and τ and E_a are the correlation time and the activation energy of the C_3 reorientation, respectively. From least-squares calculations using Eqs. 1 and 2, the following motional parameters were obtained: $C_Q = 2.80 \times 10^{10} s^{-2}$, $\tau_0 = 4.6 \times 10^{-14} s$, and $E_a = 30.7 kJ mol^{-1}$. The obtained E_a value for the $[C(ND_2)_3]^+$ ion in $[C(ND_2)_3]HgBr_3$ was a little smaller than the value $35.0 kJ mol^{-1}$ for the $[C(NH_2)_3]^+$ ion in $[C(NH_2)_3]HgBr_3$. This may show the fact that the N–D...Br hydrogen-bonding interactions are weaker than the N–H...Br ones, and the N–D...I ones are weaker than the N–H...I. This trend is consistent with the expected strengthening of N–H bond and resultant weakening of N–H...X hydrogen bond as a consequence of deuteration.¹⁴

Though the deuteration effect on T_c is not yet fully understood, Weiss et al.¹⁴ have pointed out two opposite influences on T_c in anilinium halogenides (halogen = Br and I). One is a disordering of the cations, which may cause a decrease in T_c following deuteration, because deuterated compounds may be easier to disorder than protonated ones, due to a decrease in hydrogen-bond strength. The other is a crystal stabilization effect arising from diminished torsional amplitudes expected for a deuterated ion. The former was adopted as a predominate influence in $C_6H_5ND_3X$ and $C_6D_5ND_3X$, which show ca. 6 K lowering from their order–disorder phase-transition temperatures of respective protonated compounds. It is noted that in the KH_2PO_4/KD_2PO_4 example, the D atom is more difficult to disorder than the H atom and a drastic increase of 106 K in T_c is encountered on deuteration.¹⁴ The latter was introduced to explain a quite small but definite increase (0.7 K) in the T_c of $C_6D_5NH_3Br$. Another example showing the phase transitions connected to a cation disorder may be the family of $C_6H_5NHSbX_4$ ($X = Br$ and Cl),⁹ for which T_c decreases by few degrees on deuteration. The increase in T_c in the present case of $[C(ND_2)_3]HgI_3/[C(NH_2)_3]HgI_3$ may be difficult to explain by the order–disorder of cations at the phase transitions. Therefore, we consider that the increased crystal stabilization on deuteration is responsible for the increase in T_c . This

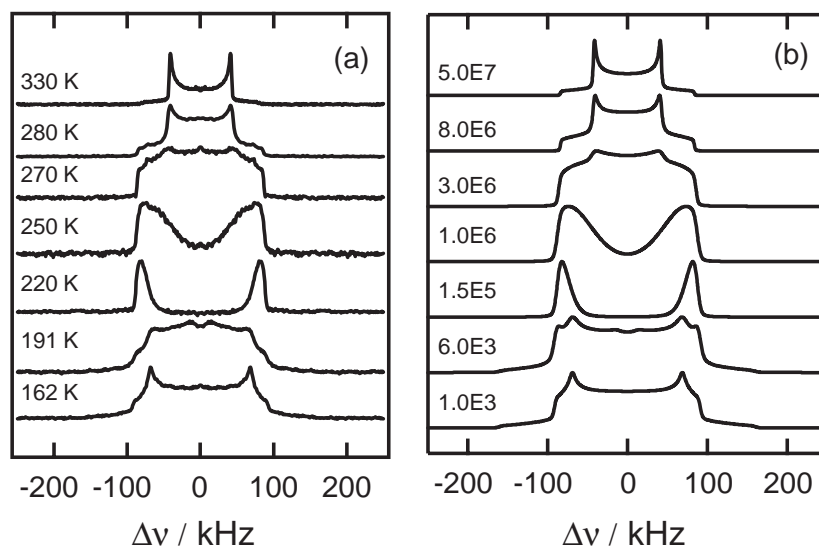


Fig. 6. (a) ^2H NMR spectra of $[\text{C}(\text{ND}_2)_3]\text{HgBr}_3$ at selected temperatures and (b) simulations under the C_3 reorientation with the rate k shown in the figure.

also suggests that the phase transition at T_{c1} (and probably at T_{c2}) is a displacive-type transition (Our preliminary crystal structure investigations of the low-temperature structures of $[\text{C}(\text{NH}_2)_3]\text{HgI}_3$ also indicate a displacive-type transition.).

^2H NMR spectra of $[\text{C}(\text{ND}_2)_3]\text{HgBr}_3$ are shown in Fig. 6, together with simulated spectra. According to the crystal-structure determinations on $[\text{C}(\text{NH}_2)_3]\text{HgBr}_3$ ² and $[\text{C}(\text{NH}_2)_3]\text{CdBr}_3$,³ the NH_2 planes of cations were found to be twisted by small angles from the plane of a coplanar CN_3 group. However, many recent structure determinations¹⁵ have shown that the guanidinium ions are found coplanar including the H atoms in the crystal structures. It seems appropriate that all atoms of the cations are situated coplanar, because the C–N bonds may have partial double bond character and both N and C atoms are expected to use sp^2 hybrid orbitals for their bonding. Therefore, we simulated the ^2H NMR spectra for the coplanar cations including the H atoms. The simulation was further carried out with C_3 reorientational motion of the $[\text{C}(\text{ND}_2)_3]^+$ cation with the reorientation rate k , because no other motion was detected by the ^2H NMR T_1 in this temperature region. The spectrum at 162 K was well explained with a rigid lattice of the $[\text{C}(\text{ND}_2)_3]^+$ ion, from which the quadrupole coupling constant (e^2Qq/h) and the asymmetry parameter (η) of the electric field gradient (EFG) for the ^2H were estimated to be 214 kHz and 0.14, respectively. This e^2Qq/h was close to 230 kHz, which has been reported for the guanidinium cation intercalated into a clay mineral.¹⁶

These simulations from 162 to 330 K suggest that the z -axis of the EFG at the rigid lattice is parallel to the D–N bond and that the y -axis is normal to the D–N–D plane, that is, the y -axis is parallel to the C_3 axis. These findings are consistent with a planar $[\text{C}(\text{ND}_2)_3]^+$ ion, including three ND_2 groups.

Figure 7 plots the reorientational rates (k) in the simulation against the inverse of the temperature. The following Arrhenius-type equation gave the best fit for the data:

$$k = 9.0(10) \times 10^{12} \text{ s}^{-1} \exp(-32(1) \text{ kJ mol}^{-1}/RT). \quad (3)$$

The calculated activation energy (32(1) kJ mol^{−1}) is consistent

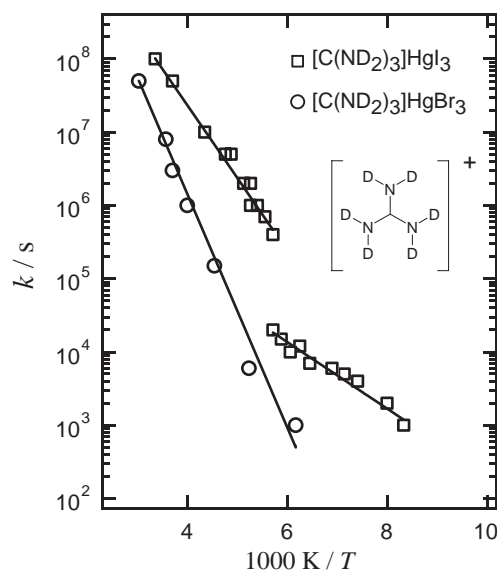


Fig. 7. Arrhenius plot of the C_3 reorientational rate k for the $[\text{C}(\text{ND}_2)_3]^+$ ions in $[\text{C}(\text{ND}_2)_3]\text{HgBr}_3$ (○) and $[\text{C}(\text{ND}_2)_3]\text{HgI}_3$ (□).

with that (30.7 kJ mol^{−1}) obtained from the above ^2H NMR T_1 measurement. The spectrum at 330 K corresponds to one with axial symmetry ($\eta = 0$), because the C_3 reorientational motion becomes much faster than the NMR line width ($k \gg 10^7 \text{ s}^{-1}$). The e^2Qq/h value at this temperature was estimated to be 112 kHz, which is ca. 8% smaller than the expected value involving pure C_3 reorientation of a planar guanidinium- d_6 ion. This reduction suggests a wobbling property of the reorientational axis. A simple consideration of such a mode may reduce e^2Qq/h to the following:

$$e^2Qq/h = (e^2Qq/h)_{\theta=0} \cdot \frac{3 \cos^2 \theta - 1}{2}, \quad (4)$$

where θ is a tilting angle of the C_3 axis from the precessional axis, and $(e^2Qq/h)_{\theta=0} = 122 \text{ kHz}$ for pure C_3 reorientation.

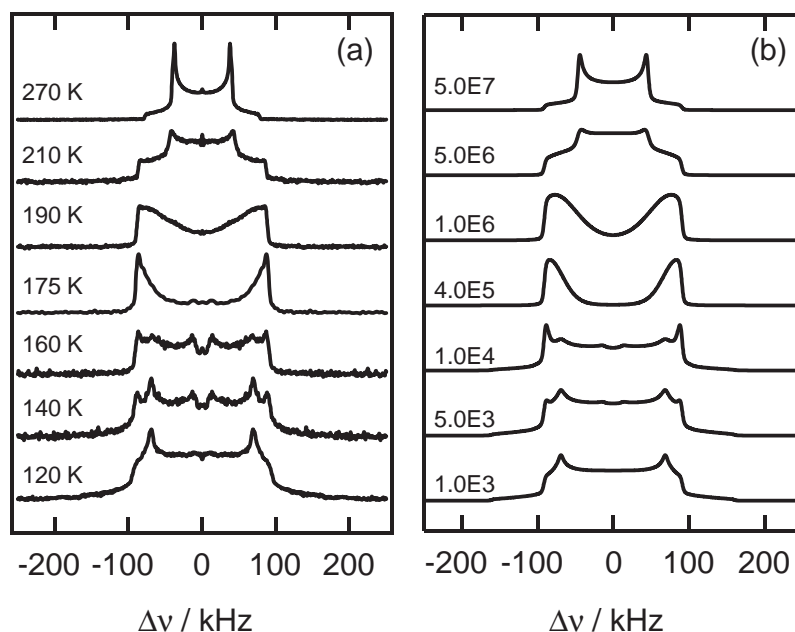


Fig. 8. (a) ^2H NMR spectra of $[\text{C}(\text{ND}_2)_3]\text{HgI}_3$ at selected temperatures and (b) simulations under the C_3 reorientation with the rate k shown in the figure.

The calculation showed a small angle tilting with $\theta = 13.5^\circ$ at 330 K.

^2H NMR spectra for $[\text{C}(\text{ND}_2)_3]\text{HgI}_3$ are shown together with the simulation in Fig. 8. In spite of the existence of phase transitions, the spectra could be reproduced successfully with the simulation using C_3 reorientational motion similar to the bromide analog. The spectrum at 120 K was well explained with a rigid lattice of the $[\text{C}(\text{ND}_2)_3]^+$ ion with $e^2Qq/h = 216$ kHz and $\eta = 0.13$, which are very close to those of the bromide analog.

The k vs. T^{-1} plot for this compound is included in Fig. 7. In accordance with the N–D...I bonds being weaker than the N–D...Br bonds as well the packing in the iodine compound being looser than the bromine one, the k values in the iodine compound were about one order larger than those in the bromine compound. No clear change was observed above and below $T_{\text{c1}}(\text{D})$ ($1000/T = 3.95$) on the k vs. T^{-1} plot. On the other hand, an abrupt drop of k was seen at the transition from the supercooled ITP to LTP. The k vs. T^{-1} plot of the iodine compound was thus best-fitted by using two Arrhenius-type equations. The activation energies were calculated to be 20(1) and 9(1) kJ mol^{-1} above ITP and at LTP, respectively. The former value seems to be consistent with the value (24.1 kJ mol^{-1}) in RTP for the protonated analog obtained from ^1H NMR T_1 , because a smaller E_a is expected for the deuterated analog as observed between $[\text{C}(\text{ND}_2)_3]\text{HgBr}_3$ and $[\text{C}(\text{NH}_2)_3]\text{HgBr}_3$. The latter value (9(1) kJ mol^{-1}) is quite small compared to the value (23.0 kJ mol^{-1}) from the ^1H NMR T_1 measurement. In the former ^1H NMR T_1 experiment, the measurements were carried out down to about 170 K, where the T_1 values became considerably long. On the other hand, the ^2H NMR spectra were measured down to 120 K, and it is thus expected that another mode of motion of the cation occurs. This slow reorientation with a low activation energy excited at LTP seems to be responsible for the disappearance

of the ^{127}I NQR lines below ca. 100 K owing to the quenching of the orientation disorder of the cation. The disappearance of the ^{81}Br NQR resonance lines of $[\text{C}(\text{NH}_2)_3]_3\text{Sb}_2\text{Br}_9$ ^{15d} occurred below ca. 150 K, for which the disorder of guanidinium cations seems also to be responsible.

The spectrum at 270 K corresponds to a typical one with axial symmetry ($\eta = 0$) with $e^2Qq/h = 101$ kHz. This value is also much smaller than $(e^2Qq/h)_{\theta=0} = 122$ kHz expected for simple C_3 reorientation. Equation 4 gave the tilting angle 20° , which is much larger than that calculated for the bromide analog.

Conclusion

On deuteration, the phase-transition temperatures of $[\text{C}(\text{NH}_2)_3]\text{HgI}_3$ shifted to a higher temperature by several degrees. The distinctive NQR frequency shifts due to deuteration were found in ITP of the iodine compound. The ^2H NMR spectra were well explained by invoking C_3 reorientation with wobbling of the $[\text{C}(\text{ND}_2)_3]^+$ ion. From both the ^2H NMR T_1 and ^2H NMR measurements, the activation energy of the reorientational motion of guanidinium cations decreased upon deuteration, which may indicate the weaker interaction of N–D...X than N–H...X. The phase transitions in $[\text{C}(\text{NH}_2)_3]\text{HgI}_3$ were thought to be not an order–disorder-type transition but a displacive one. The existence of the reorientational motion with small activation energy in LTP of $[\text{C}(\text{ND}_2)_3]\text{HgI}_3$ from the present ^2H NMR spectra may be responsible for the disappearance of the ^{127}I NQR lines below ca. 100 K, because of quenching of a possible orientation disorder of the cation.

References

- 1 See e.g. a) R. Jakubas, L. Sobczyk, *Phase Transitions* **1990**, *20*, 163. b) L. Sobczyk, R. Jakubas, J. Zaleski, *Pol. J. Chem.* **1997**, *71*, 265.
- 2 H. Terao, M. Hashimoto, S. Hashimoto, Y. Furukawa,

Z. Naturforsch., A: Phys. Sci. **2000**, 55, 230.

3 V. G. Krishnan, S.-q. Dou, Al. Weiss, *Z. Naturforsch., A: Phys. Sci.* **1991**, 46, 1063.

4 R. G. Barnes, J. W. Bloom, *J. Chem. Phys.* **1972**, 57, 3082.

5 G. C. Pimentel, A. L. McClellan, *The Hydrogen Bond*, Freeman, **1960**.

6 I. Pabst, J. W. Bats, H. Fuess, *Acta Crystallogr., Sect. B* **1990**, 46, 503.

7 H. Terao, T. Okuda, A. Minami T. Matsumoto, Y. Takeda, *Z. Naturforsch., A: Phys. Sci.* **1992**, 47, 99.

8 H. Terao, T. Okuda, K. Koto, S.-q. Dou, Al. Weiss, *Z. Naturforsch., A: Phys. Sci.* **1994**, 49, 202.

9 See, e.g. a) T. Okuda, K. Yamada, H. Ishihara, M. Hiura, S. Gima, H. Negita, *J. Chem. Soc., Chem. Commun.* **1981**, 979. b) T. Okuda, Y. Aihara, N. Tanaka, K. Yamada, S. Ichiba, *J. Chem. Soc., Dalton Trans.* **1989**, 631. c) K. Yamada, T. Ohtani, S. Shirakawa, H. Ohki, T. Okuda, T. Kamiyama, K. Oikawa, *Z. Naturforsch., A: Phys. Sci.* **1996**, 51, 739.

10 Z. Pajak, M. Grottel, A. E. Koziol, *J. Chem. Soc., Faraday*

Trans. **2** **1982**, 78, 1529.

11 S. Gima, Y. Furukawa, D. Nakamura, *Ber. Bunsen-Ges. Phys. Chem.* **1984**, 88, 939.

12 M. Grottel, Z. Pajak, J. Zaleski, *Solid State Commun.* **2001**, 120, 119.

13 Y. Furukawa, H. Terao, *Z. Naturforsch., A: Phys. Sci.* **2002**, 57, 399.

14 a) G. Fecher, Al. Weiss, *Ber. Bunsen-Ges. Phys. Chem.* **1986**, 90, 10. b) W. Pies, Al. Weiss, *Bull. Chem. Soc. Jpn.* **1978**, 51, 1051.

15 See e.g. a) J. Zaleski, A. Pietraszko, *J. Mol. Struct.* **1994**, 327, 287. b) J. Zaleski, A. Pietraszko, *Z. Naturforsch., A: Phys. Sci.* **1994**, 49, 895. c) R. Jakubas, P. Ciapala, A. Pietraszko, J. Zaleski, J. Kusz, *J. Phys. Chem. Solids* **1998**, 59, 1309. d) H. Terao, Y. Furukawa, S. Miki, F. Tajima, M. Hashimoto, *Hyperfine Interact.* **2004**, 159, 211.

16 M. Yamauchi, S. Ishimaru, R. Ikeda, *Chem. Lett.* **2003**, 32, 976.